communications biology

A Nature Portfolio journal

Article

https://doi.org/10.1038/s42003-025-07679-8

Central amygdala somatostatin neurons modulate stress-induced sleep-onset insomnia

Wei Yao[1,5], Shu-Xin Huang[1,5], Lei Zhang[2], Zhang-Shu Li[3], Ding-Yuan Huang[3], Kai-Qi Huang[3], Zi-Xuan Huang[3], Li-Wei Nian[3], Jia-Lu Li[3], Li Chen[2,4] ✉ & Ping Cai[1] ✉

Sleep-onset insomnia, characterized by difficulty falling asleep, is linked to increased health risks. Previous studies have shown that the central amygdala (CeA) plays a crucial role in stress regulation, with the somatostatin neurons in the CeA (CeA^{SST+}) involved in adaptive stress responses. However, the role of CeA^{SST+} neurons in stress-induced sleep-onset insomnia remains unclear. In this study, we found that the activity of CeA^{SST+} neurons is closely associated with stressful events using fiber photometry in mice. Acute optogenetic activation of CeA^{SST+} neurons induced a rapid transition from non-rapid eye movement (NREM) sleep to wakefulness. Semi-chronic optogenetic and chemogenetic activation of CeA^{SST+} neurons led to prolonged sleep-onset latency and increased wakefulness. Chemogenetic inhibition of these neurons ameliorated sleep-onset insomnia induced by stressful stimuli, but did not affect sleep-wake behavior under physiological conditions. Collectively, our results suggested that CeA^{SST+} neurons are a key neural substrate for modulating stress-induced sleep-onset insomnia, without influencing physiological sleep. These findings highlight CeA^{SST+} neurons as a promising target for treating stress-related sleep-onset insomnia in clinical practice.

Insomnia, one of the most prevalent sleep disorders, is characterized by difficulty falling asleep, difficulty maintaining sleep, or early morning awakening[1], and is hence categorized into sleep-onset insomnia, sleep maintenance insomnia and early morning awakening insomnia, correspondingly[2]. People with sleep-onset insomnia periodically or permanently take more than 30 min to fall asleep at night[3]. Difficulty falling asleep will lead to reduced nocturnal sleep time and increase diurnal sleepiness, and affect the progression and severity of insomnia[4]. However, the underlying neural mechanisms of sleep-onset insomnia remain unknown.

Stress is a major etiology of sleep-onset insomnia, and prolonged sleep latency is a common manifestation under or after stress in both humans and animals. Stress-induced sleep-onset insomnia is detrimental to the health of human beings and adversely affects public life, increasing the risk of negative outcomes including heart disease, stroke, and all-cause mortality[5–7]. Dissecting the neural circuit of stress-induced sleep-onset insomnia is critical for the advancement of insomnia treatment. The central amygdala (CeA), a pivotal hub in the regulation of stress response, has been implicated in the sleep-onset insomnia. Cano and colleagues observed that cage-change stress significantly lengthened the sleep latency of rats and increased the c-fos expression in the CeA[8]. Combined lesions of the CeA and the bed nucleus of the stria terminalis alleviated the prolongation of sleep latency in the stress condition and attenuated the stress-induced sleep-onset insomnia in cage change model[8]. These findings indicate that the CeA may serve as a neural substrate in modulating stress-related sleep-onset insomnia.

The CeA, a heterogeneous nucleus, mainly composed of GABAergic neurons which comprise diverse neural subtypes characterized by gene markers, such as protein kinase C δ neurons, somatostatin (SST) neurons, corticotropin-releasing hormone (CRH) neurons, neurotensin (NTS) neurons, etc[9,10]. Results from two different labs demonstrated that the GABAergic neurons in the CeA modulate cataplexy, but are not critical for sleep regulation[11,12]. The study of Ma et al. showed that optogenetic activation of NTS+ neurons in the CeA enhanced NREM sleep, while inhibition of these neurons suppressed NREM sleep[10]. However, the specific neuronal subtype of in the CeA responsible for sleep-onset insomnia remains unclear. As one of the main neuronal subpopulations in the CeA, SST neurons have been involved in the regulation of the stress response[13,14]. Rodent studies have shown that acute exposure to potential predators led to the upregulation of SST receptor 2 mRNA expression in the amygdala[15].

[1]Fujian Province Key Laboratory of Environment and Health, School of Public Health, Fujian Medical University, Fuzhou, Fujian, China. [2]Department of Pharmacology, School of Pharmacy, Fujian Medical University, Fuzhou, Fujian, China. [3]School of Basic Medical Sciences, Fujian Medical University, Fuzhou, Fujian, China. [4]Fujian Key Laboratory of Drug Target Discovery and Structural and Functional Research, Fujian Medical University, Fuzhou, Fujian, China. [5]These authors contributed equally: Wei Yao, Shu-Xin Huang. ✉e-mail: lichen01005@163.com; caipingfjmu@163.com

Moreover, optogenetic activation of SST neurons in the CeA (CeA^{SST+}) induced anxiety-like behavior in mice, while inhibition of these neurons reduced anxiety-like behavior triggered by restraint stress[16]. Based on this evidence, we hypothesized that CeA^{SST+} neurons may be crucial in regulating stress-induced sleep-onset insomnia.

In this study, we showed that the Ca^{2+} activity of CeA^{SST+} neurons was increased in response to various stressors, including restraint, rat bedding, air puff, and cage change challenge. Furthermore, activation of CeA^{SST+} neurons led to increased pupil size, respiratory rate and anxiety-like behavior, suggesting their involvement in stress regulation. Subsequently, acute optogenetic activation of CeA^{SST+} neurons induced a rapid transition from NREM sleep to wakefulness, while semi-chronic optogenetic activation of CeA^{SST+} neurons prolonged sleep-onset latency but not maintained long-term wakefulness in mice. Similarly, chemogenetic activation of CeA^{SST+} neurons delayed sleep-onset. Interestingly, chemogenetic inhibition of CeA^{SST+} neurons alleviated sleep-onset insomnia induced by cage change challenge and restraint stress, but not alter sleep-wake behavior under physiological conditions. Collectively, our findings indicate that CeA^{SST+} neurons play a crucial role in modulating acute stress-induced sleep-onset insomnia, but not influence physiological sleep. In the future, therapeutic interventions targeting CeA^{SST+} neurons may offer a promising avenue for the effective treatment of acute stress-related sleep insomnia without disrupting physiological sleep.

Results

Acute stressors activates CeA^{SST+} neurons

The CeA plays an important role in the regulation of fear memory and anxiety[16–18], but the activity of CeA^{SST+} neurons responding to different stressors has not been clearly elucidated. In order to directly measure the temporal dynamics of CeA^{SST+} neurons in response to stressors, we injected AAV encoding Cre-dependent Ca^{2+} indicator (AAV-EF1a-DIO-jGCamp7s) into the CeA of SST-Cre mice (Fig. 1A). At the same time, optical fibers were implanted above the CeA to obtain the population Ca^{2+} fluorescence of CeA^{SST+} neurons (Fig. 1B). About 4 weeks later, the mice were connected to a fiber photometry system to monitor the real-time jGCamp7s signals of CeA^{SST+} neurons (Fig. 1C). After that, we exposed the mice to different types of stressors. In the physical restraint test, the mice were artificially restricted for 5 s (Fig. 1D). The fiber photometry recording results showed that the Ca^{2+} activity of CeA^{SST+} neurons increased significantly when the mice were restrained (Fig. 1E, F and Supplementary Fig. 1A, Baseline: 1.384 ± 0.1563%; Restraint: 5.261 ± 0.4001%). Then, we exposed the mice to more stressful stimuli types, such as rat bedding and air puff stress (Fig. 1G, J). The Ca^{2+} activity of CeA^{SST+} neurons also increased significantly when the mice were exposed to rat bedding (Fig. 1H, I and Supplementary Fig. 1B, Baseline: 2.118 ± 0.2010%; Rat bedding: 6.598 ± 0.2947%) and air puff stress (Fig. 1K, L and Supplementary Fig. 1C, Baseline: 1.193 ± 0.1132%; Air puff: 9.318 ± 0.5100%). In the cage change challenge, the mice were transferred from their home cage to another cage where other mice lived for at least 7 days (Fig. 1M). The population activity of CeA^{SST+} neurons increased significantly when the mice were transferred into the cages filled with dirty bedding (Fig. 1N, O and Supplementary Fig. 1D, Baseline: 4.537 ± 0.4042%; Dirty cage: 17.53 ± 2.905%). These results showed that CeA^{SST+} neurons are activated by acute stressors.

Then, in order to further verify the relationship between CeA^{SST+} neuron activity and stress reaction, we evaluated the physiological and behavioral indicators of stress following the activation of CeA^{SST+} neurons by optogenetics. Firstly, we measured the fluctuations of pupil size and respiratory rate during optogenetic stimulation in mice (Supplementary Fig. 2A, E). Our results showed that optogenetic stimulation of CeA^{SST+} neurons significantly increased pupil size and respiratory rate compared to pre-stimulation (Supplementary Fig. 2B–D, F, G, Pre vs. Stim; Normalized pupil size in control group: 0.9568 ± 0.03363 vs. 0.8824 ± 0.07119; ChR2 group: 0.9620 ± 0.03779 vs. 1.327 ± 0.05678; Pre vs. Stim; Respiratory rate in control group: 81.58 ± 3.097 N/min vs. 78.89 ± 3.467 N/min; ChR2 group: 87.8 ± 6.537 N/min vs. 106.7 ± 6.926 N/min). In addition, we tested the behavioral responses induced by the optogenetic activation of CeA^{SST+} neurons in open field and elevated plus maze (Supplementary Fig. 3A, D). In the open field test, mice spent less time in the center, stayed longer time in periphery and didn't change the total distance of movement in the open field following blue light stimulation compared to yellow light stimulation (Supplementary Fig. 3B, C, Yellow light vs. Blue light; Center: 15.12 ± 2.535 s vs. 3.838 ± 1.189 s; Periphery: 284.9 ± 2.535 s vs. 296.2 ± 1.189 s; Total distance: 1238 ± 167.5 cm vs. 1118 ± 91.01 cm). In the elevated plus maze test, mice stayed longer in the closed arms, spent less time in the open arms and didn't change the total distance of movement following blue light stimulation compared to yellow light stimulation (Supplementary Fig. 3E, F, Yellow light vs. Blue light; Open arms: 38.56 ± 5.054 s vs. 13.63 ± 3.637 s; Closed arms: 239.8 ± 9.638 s vs. 277.3 ± 4.833 s; Total distance: 756.2 ± 97.39 cm vs. 643.4 ± 57.58 cm). These results together showed that activation of CeA^{SST+} neurons produced stress reaction and anxiety-like behavior, which suggested that these neurons might play an important role in acute stress-induced disturbance of sleep-wake behavior.

Optogenetic activation of CeA^{SST+} neurons prolongs sleep-onset latency, but not maintains long-term wakefulness

It has been reported that some substrates of the wakefulness-promoting system are activated by stress[19]. After showing that the CeA^{SST+} neurons regulate the stress reaction, we hypothesized that CeA^{SST+} neurons are involved in the regulation of sleep-wake behavior. We conducted EEG/EMG recordings while manipulating the activity of CeA^{SST+} neurons using optogenetic methods. We injected AAV encoding channelrhodopsin-2 conjugated with mCherry (AAV-EF1a-DIO-hChR2(H134R)-mCherry) into the CeA, optical fibers were bilaterally implanted above the CeA to stimulate the soma of CeA^{SST+} neurons (Fig. 2A). After four weeks of transfection, red fluorescence was strongly expressed in the CeA (Fig. 2B). To further demonstrate that the neurons expressing AAV-EF1a-DIO-hChR2(H134R)-mCherry are activated by optogenetic stimulation, we detected the expression of c-fos after delivering blue light (473 nm) to the CeA. Immunofluorescence results showed that blue light stimulation drove higher levels of c-fos expression in the CeA compared with yellow light stimulation (Supplementary Fig. 4), which demonstrated that CeA^{SST+} neurons were effectively activated by blue light.

Then, we evaluated the effects of acute activation of CeA^{SST+} neurons on sleep-wake behavior. Four weeks after the virus was transfected, the mice were connected to the sleep recording system (Fig. 2C). We performed acute light stimulation at different frequency (5, 10, 20, and 40 Hz) when mice entered the NREM stage for at least 20 s. We assessed the latency of transition from NREM sleep to wakefulness and the transition probability. Our results showed that higher frequency blue light stimulation (10, 20 or 40 Hz) significantly reduced the latency of NREM-Wake transition compared to yellow light stimulation (Supplementary Fig. 5A, Blue light vs. Yellow light; Base: 60.00 ± 0 s vs. 60.00 ± 0 s; 5 Hz: 44.88 ± 2.885 s vs. 60 ± 0 s; 10 Hz: 32.71 ± 4.211 s vs. 60.00 ± 0 s; 20 Hz: 11.63 ± 2.410 s vs. 60.00 ± 0 s; 40 Hz: 5.417 ± 0.745 s vs. 60.00 ± 0 s), and increased the probability of the NREM-Wake transition in a frequency-dependent manner (Supplementary Fig. 5B). We took the optogenetic parameters of 20 Hz based on previous studies[20,21]. When light stimulation was applied at 20 Hz, blue light effectively changed the EEG power spectral compared to yellow light (Fig. 2D) and induced 100% NREM-Wake transition (Fig. 2E, F). These results indicated the causal role for CeA^{SST+} neurons in initiating wakefulness.

Moreover, we investigated the effect of 1-h and 3-h optogenetic activation of CeA^{SST+} neurons on sleep latency and wakefulness maintenance. Blue or yellow light stimulation began at ZT 2 during the light period and lasted for 1 h (Fig. 2G). The experimental results showed that 1-h blue light stimulation significantly increased sleep-onset latency (Fig. 2H, Yellow light vs. Blue light; 1.567 ± 1.362 min vs. 35.05 ± 6.037 min) and altered the sleep architecture of the mice, which was characterized by decreased EEG amplitude and increased EMG activity, while yellow light stimulation did not significantly affect EEG signals (Fig. 2I). Blue light stimulation

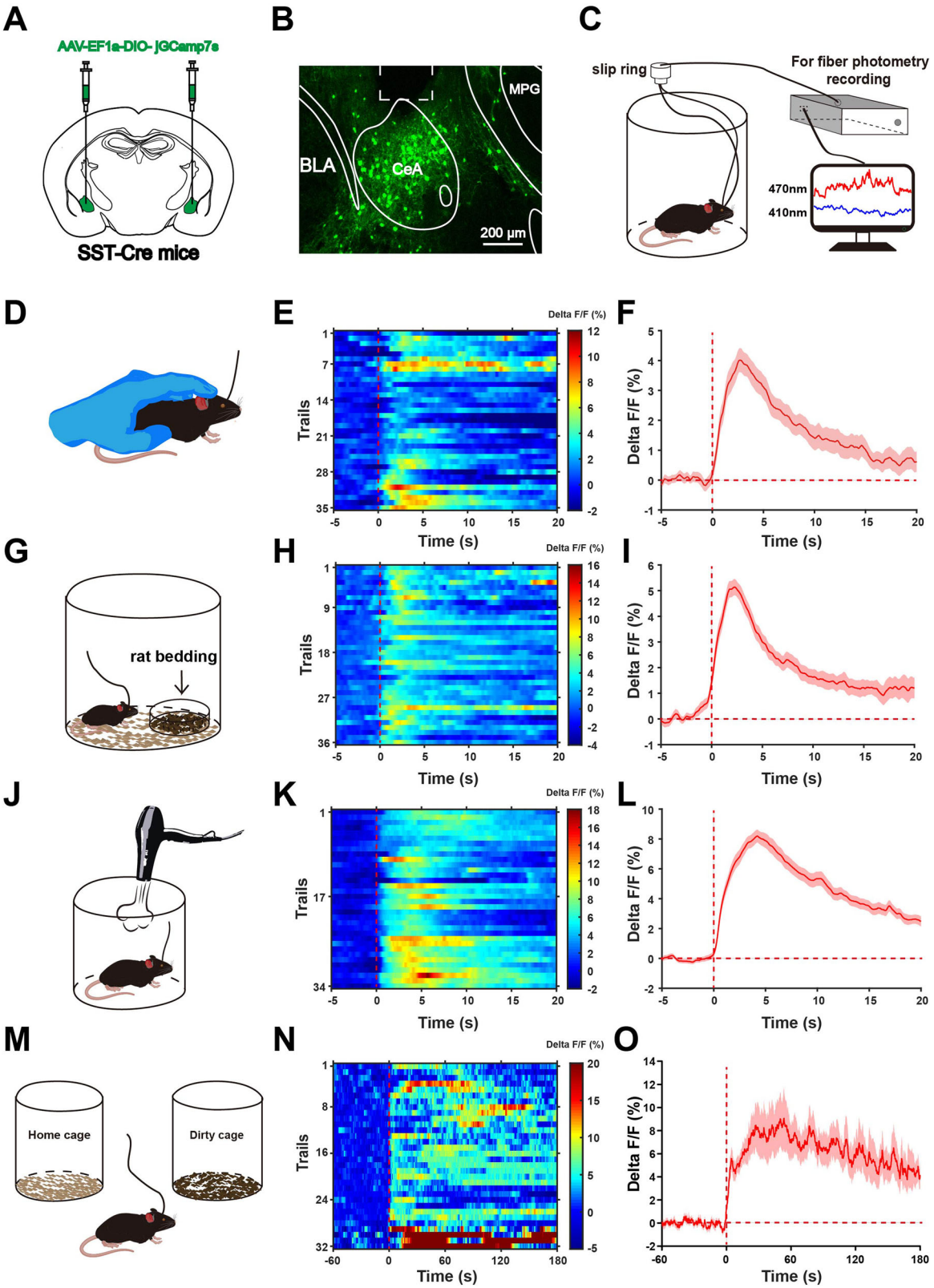

Fig. 1 | The dynamic activity of CeA^{SST+} neurons in response to acute stress. **A** Schematic diagram of AAV-EF1a-DIO-jGCamp7s injection into the CeA of SST-Cre mice. **B** Representative image showing the expression of AAV-EF1a-DIO-jGCamp7s in the CeA of SST-Cre mice. Scale bars: 200 μm. **C** Schematic of experimental setup of fiber photometry recording. Schematic of physical restraint (**D**), heatmap (**E**), and peri-event plot of the average Ca^{2+} transients (**F**) associated with physical restraint. The color scale indicates the $\Delta F/F$ (%). $n = 35$ trials from 4 mice. Schematic of rat bedding stress (**G**), heatmap (**H**), and peri-event plot of the average Ca^{2+} transients (**I**) associated with rat bedding stress. The color scale indicates the $\Delta F/F$ (%). $n = 36$ trials from 4 mice. Schematic of air puff stress (**J**), heatmap (**K**) and peri-event plot of the average Ca^{2+} transients (**L**) associated with air puff stress. The color scale indicates the $^{\triangle}F/F$ (%). $n = 34$ trials from 4 mice. Schematic of cage change challenge (**M**), heatmap (**N**) and peri-event plot of the average Ca^{2+} transients (**O**) associated with cage change challenge. The color scale indicates the $\Delta F/F$ (%). $n = 32$ trials from 4 mice. Red vertical dashed lines indicate the time points of introducing different stressors.

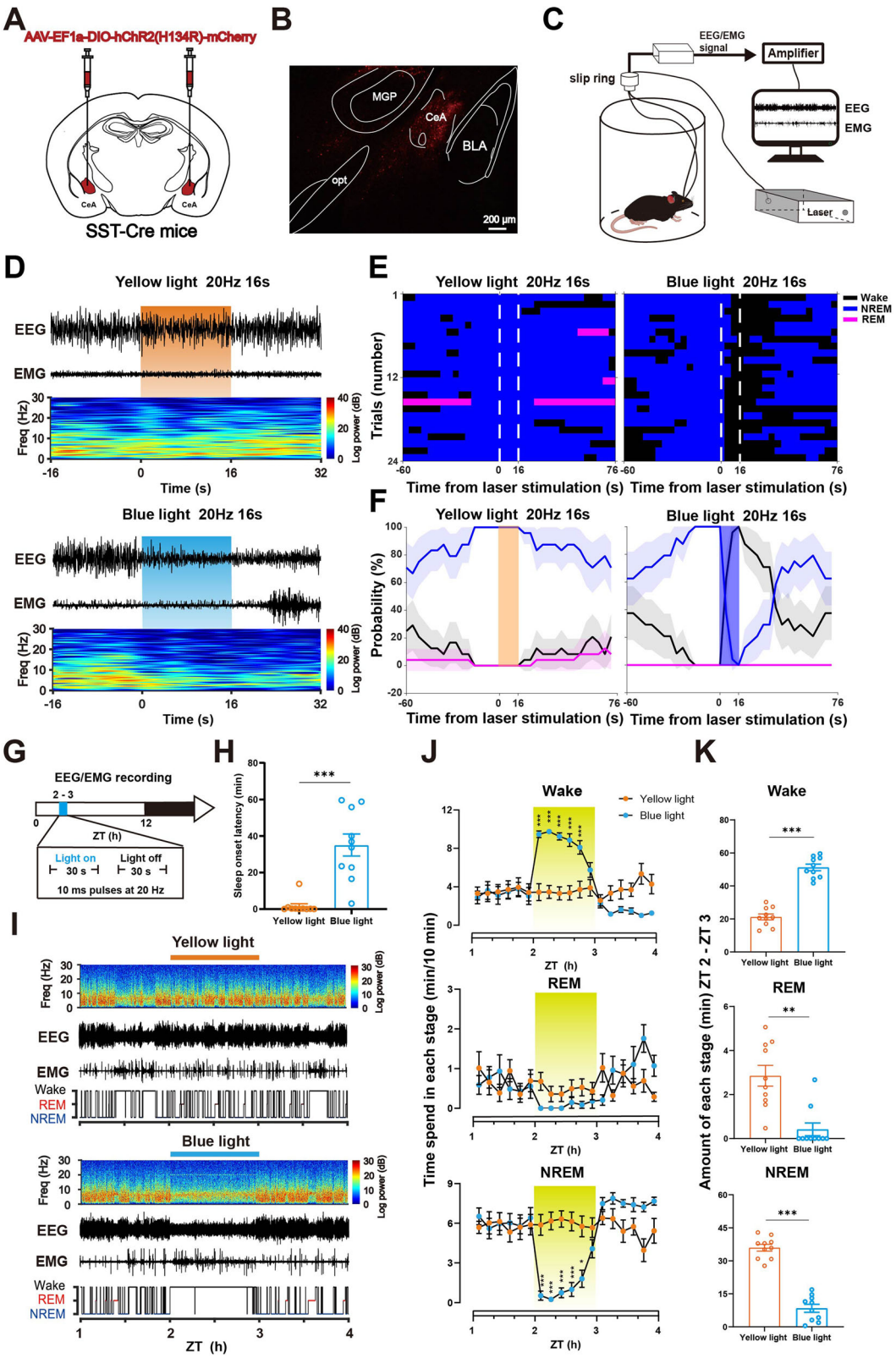

significantly increased the total amount of wakefulness, and decreased the total amount of NREM and REM sleep during ZT 2 - ZT 3 (Fig. 2J, K, Yellow light vs. Blue light; Wake: 21.20 ± 1.807 min vs. 51.19 ± 1.992 min; REM: 2.853 ± 0.4740 min vs. 0.4140 ± 0.2901 min NREM: 35.95 ± 1.553 min vs. 8.396 ± 1.827 min). We further examined the effect of 3-h optogenetic stimulation on sleep-wake behavior (Fig. 3A). Our results showed that blue light stimulation significantly increased the sleep-onset latency compared to yellow light stimulation (Fig. 3B, Yellow light vs. Blue light; 3.837 ± 2.545 min vs. 44.86 ± 6.354 min) and promoted wakefulness in mice only during the first hour (Fig. 3C). Blue light stimulation significantly increased the total amount of wakefulness, and decreased the total amount of NREM sleep during ZT 2 - ZT 3 (Fig. 3D, Yellow light vs. Blue light; Wake:

Fig. 2 | Effects of acute and 1-hour optogenetic activation of CeA $^{SST+}$ neurons on sleep-wake behavior in mice. A Schematic diagram of AAV-EF1a-DIO-hChR2(H134R)-mCherry injection into the CeA of SST-Cre mice. **B** Representative image showing the expression of AAV-EF1a-DIO-hChR2(H134R)-mCherry in the CeA. Scale bars: 200 μm. **C** Schematic diagram of acute optogenetic stimulation in sleep-wake behavior experiment. **D** The typical examples of the NREM sleep to wakefulness transition during the yellow (top) or blue (bottom) light stimulation. **E** Sleep stages after yellow (left) or blue (right) light stimulation in AAV-EF1a-DIO-hChR2(H134R)-mCherry mice. **F** Possibility of NREM sleep, REM sleep and wakefulness before, during and after yellow (left) or blue (right) light stimulation. **G** Timeline of sleep-wake behavior recording experiment with 1-h optogenetic stimulation. Mice were stimulated with light (10 ms, 20 Hz, 30 s on, 30 s off) from ZT 2 to ZT 3. **H** Sleep latency after yellow or blue light stimulation. Paired t-test ($n = 10$). **I** Representative EEG power spectra, EEG/EMG traces and hypnogram after yellow light (top) or blue light (bottom) stimulation. **J** Time course of wakefulness, NREM sleep, and REM sleep following yellow and blue light stimulation of the CeA^{SST+} neurons from ZT 2 to ZT 3. Two-way repeated-measures ANOVA, Bonferroni post-hoc comparison ($n = 10$). **K** Total time spent in each stage during the 1-h exposure to yellow or blue light stimulation. Paired t-test ($n = 10$).

26.61 ± 2.855 min vs. 50.89 ± 3.043 min; REM: 2.547 ± 0.5040 min vs. 0.8467 ± 0.4316 min NREM: 30.83 ± 2.649 min vs. 8.267 ± 2.676 min), but did not significantly change the amount of each stage during ZT 3 - ZT 5 (Fig. 3E, Yellow light vs. Blue light; Wake: 50.82 ± 6.309 min vs. 40.67 ± 2.561 min; REM: 6.813 ± 1.364 min vs. 7.860 ± 0.9646 min; NREM: 62.39 ± 5.096 min vs. 71.49 ± 2.006 min).The numbers of different episode lengths of wakefulness, NREM sleep and REM sleep and the average duration of each state also did not change during ZT 3 - 5 exposure to blue light stimulation (Fig. 3F–I). Our results demonstrated that optogenetic activation of CeA^{SST+} neurons contributes to prolonging sleep-onset latency, but not maintaining long-term wakefulness.

Chemogenetic activation of CeA^{SST+} induces sleep-onset insomnia in mice

Next, we adapted chemogenetics, which has long-term effects, to check whether activation of CeA^{SST+} neurons only affects sleep-onset latency or also maintains wakefulness. We injected AAV-hSyn-DIO-hM3D(Gq)-mCherry into the CeA of SST-Cre mice and implanted electrode to record the EEG and EMG signals (Fig. 4A). Four weeks after virus injection, red fluorescence was potently expressed in the CeA (Fig. 4B), indicating strong expression of hM3D(Gq) receptors in the CeA. In addition, we examined the expression of c-fos protein in the CeA after intraperitoneal injection of vehicle or 1 mg/kg CNO. The results showed that c-fos was strongly expressed in the CNO group, and almost not expressed in the vehicle group (Supplementary Fig. 6), which suggests the activation of CeA^{SST+} neurons by chemogenetics. After 7 days of diurnal rhythm adaptation, the mice were connected to the sleep recording system. EEG/EMG recording began at ZT 0, and vehicle or 1 mg/kg CNO was injected intraperitoneally at ZT 2 during the light period (Fig. 4C). Our results showed that CNO injection significantly increased the sleep-onset latency (Fig. 4D, Vehicle vs. CNO, 18.53 ± 3.446 min vs. 69.61 ± 7.705 min) and altered the EEG activity, which was characterized by decreased EEG amplitude and increased EMG activity, while there was no significant change after the vehicle injection (Fig. 4E). Time-course analysis showed that chemogenetic activation of CeA^{SST+} neurons robustly increased the time spent in wakefulness, and concomitantly decreased the time of NREM and REM sleep for 1 h, compared with vehicle treatment (Fig. 4F). However, there was no difference in the total amount of each stage during ZT 3 - ZT 6 (Fig. 4G, Vehicle vs. CNO; Wake: 65.19 ± 6.868 min vs. 67.23 ± 7.671 min; REM: 13.83 ± 1.625 min vs. 12.16 ± 2.332 min; NREM: 101.0 ± 5.836 min vs. 100.6 ± 6.457 min). In addition, the numbers of episodes and the average episode durations of wakefulness, NREM sleep and REM sleep also did not significantly change during ZT 3 - 6 after CNO injection (Fig. 4H–K). To rule out the effect of CNO on sleep-wake behavior, we injected AAV-hSyn-DIO-hM3D(Gq)-mCherry on bilateral sides of the CeA in wild-type mice, and intraperitoneal injection of 1 mg/kg CNO had effects on sleep-wake architecture (Supplementary Fig. 7A–C). These results indicated that chemogenetic activation of CeA^{SST+} neurons increases the latency of sleep-onset and wakefulness amount for 1 h, but not maintains wakefulness.

Chemogenetic inhibition of CeA^{SST+} neurons does not change the sleep architecture of mice in physiological conditions

Then, we attempted to investigate whether CeA^{SST+} neurons were involved in regulation of spontaneous sleep-wake behavior. First, we monitored the jGCamp7s signaling of CeA^{SST+} neurons during spontaneous sleep-wake behavior. The mice were connected to the EEG/EMG recording system and fiber photometry recording system for recording EEG/EMG and jGCamp7s signals simultaneously (Fig. 5A). We analysed the Ca^{2+} activity of CeA^{SST+} neurons across spontaneous sleep-wake transition, and found that the Ca^{2+} activity did not change significantly during spontaneous sleep-wake transition (Fig. 5B, C, NREM: 2.284 ± 0.2946%; Wake: 2.227 ± 0.6848% REM: 2.371 ± 0.4433%). There was no significant change in Ca^{2+} activity during the transition of Wake-NREM, NREM-Wake, NREM-REM and REM-Wake (Fig. 5D–G).

Further, we adopted chemogenetic methods to explore the effect of inhibiting CeA^{SST+} neurons in physiological sleep-wake behavior. We injected AAV-hSyn-DIO-hM4D(Gi)-mCherry into the CeA of SST-Cre mice to selectively express the inhibitory receptor in CeA^{SST+} neurons (Fig. 6A). After AAV-hSyn-DIO-hM4D(Gi)-mCherry was strongly expressed in CeA (Fig. 6B), vehicle or 1 mg/kg CNO was intraperitoneally injected at ZT 2. The results showed that there was no significant change in sleep latency (Fig. 6C, Vehicle vs. CNO, 12.97 ± 2.915 min vs. 17.96 ± 3.651 min), and no significant change in EEG/EMG signals (Fig. 6D) after the vehicle and the CNO administration. There were also no significant change difference in the amount of wakefulness, NREM sleep and REM sleep (Fig. 6E, F). These findings collectively indicated that the CeA^{SST+} neurons are not necessary for wakefulness under physiological conditions. To clarify the potential non-specific effects of CNO on physiological sleep, we conducted a control experiment, in which AAV-hSyn-DIO-hM4D(Gi)-mCherry was injected into the CeA of wild-type mice. We didn't find significant change in sleep architecture between the CNO and vehicle groups. Additionally, there were no significant change in the EEG power spectra between this two groups (Supplementary Fig. 8A-C).

Chemogenetic inhibition of CeA^{SST+} neurons alleviates the sleep-onset insomnia

Evidence suggests that stressors increase the onset of sleep insomnia[22,23]. After investigating the role of CeA^{SST+} neurons in sleep-wake regulation under physiological conditions, we then explored whether CeA^{SST+} neurons were involved in the regulation of acute stress-induced sleep-onset insomnia. First, we tested the effects of the acute stress stimuli on sleep-wake behavior. In the cage change challenge, the mice are transferred to a dirty cage where other mice had lived for at least 7 days at ZT 0 (Supplementary Fig. 9A, B). The results showed that the sleep latency of the mice in the dirty cage was significantly increased compared to those in their own home cage (Supplementary Fig. 9C, Baseline: 19.57 ± 4.716 min; Dirty cage: 89.69 ± 21.54 min), and the EEG amplitude decreased significantly and EMG activity increased during ZT 0 - ZT 2 (Supplementary Fig. 9D). The amount of wakefulness increased significantly, at the expense of a decrease in NREM and REM sleep during ZT 0 - ZT 2 (Supplementary Fig. 9E). The results implicated that the cage change challenge induced sleep-onset insomnia in mice.

Next, we attempted to determine the role of CeA^{SST+} neurons in sleep-onset insomnia induced by acute cage change stress. The SST-Cre mice expressing AAV-hSyn-DIO-hM4D(Gi)-mCherry in the CeA were intraperitoneally injected with vehicle or 1 mg/kg CNO. Half an hour later, they were transferred into a dirty cage at ZT 0 (Fig. 7A). The sleep latency was reduced in the CNO treated mice compared to the vehicle treated mice

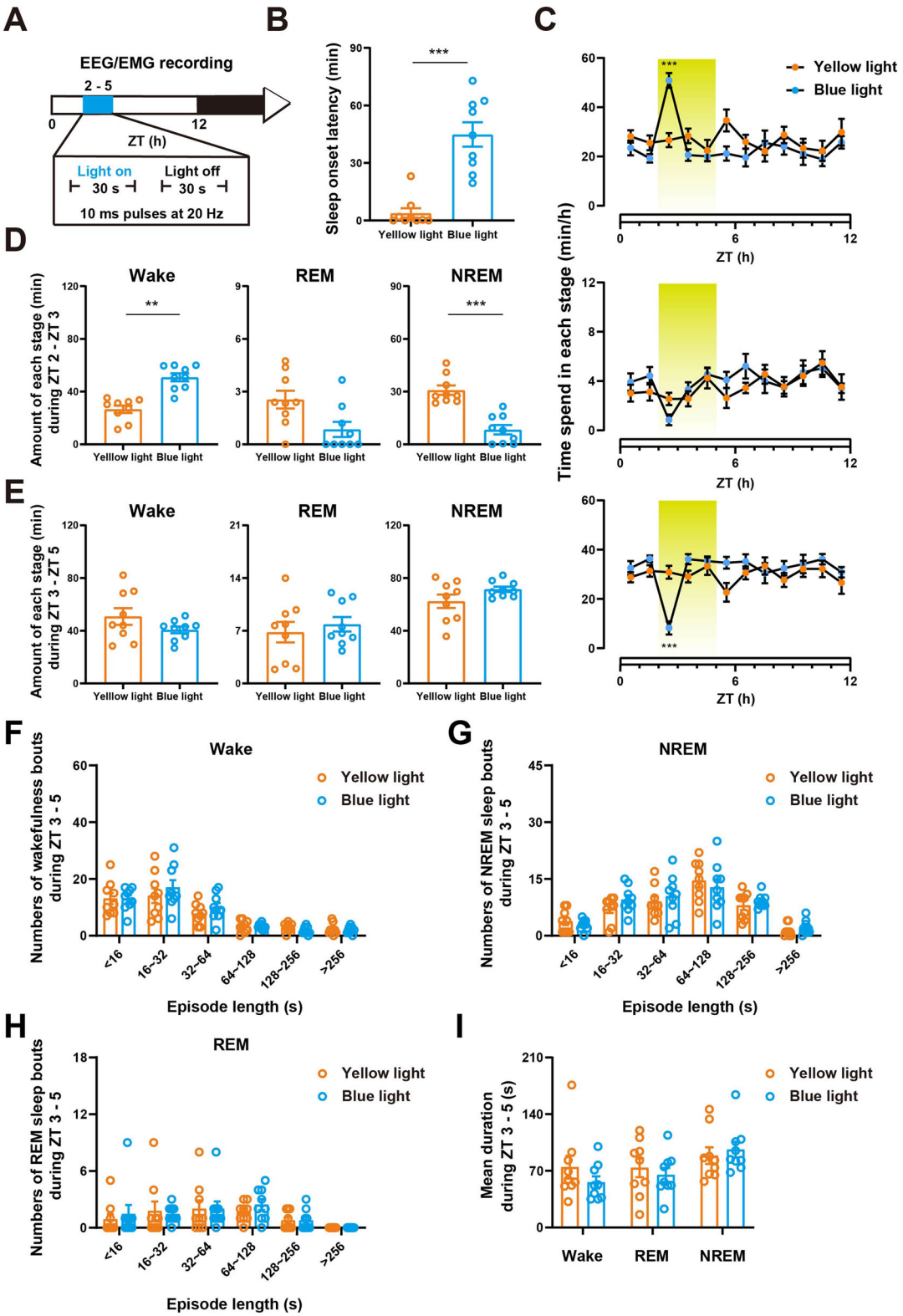

Fig. 3 | Effects of 3-hour optogenetic activation of CeA $^{SST+}$ neurons on sleep-wake behavior in mice. **A** Timeline of sleep-wake behavior recording experiment with 3-h optogenetic stimulation. Mice were stimulated with light (10 ms, 20 Hz, 30 s on, 30 s off) from ZT 2 to ZT 5. **B** Sleep latency after yellow or blue light stimulation. Paired t-test ($n = 9$). **C** Time course of wakefulness, NREM sleep, and REM sleep following yellow and blue light stimulation of the CeA^{SST+} neurons from ZT 2 to ZT 5. Two-way repeated-measures ANOVA, Bonferroni post-hoc comparison ($n = 9$). **D** Total time spent in each stage during the ZT 2 - ZT 3 exposure to yellow or blue light stimulation. Paired t-test ($n = 9$). **E** Total time spent in each stage during the ZT 3 - ZT 5 exposure to yellow or blue light stimulation. Paired t-test ($n = 9$). The numbers of different episode length including wakefulness (**F**), NREM sleep (**G**) and REM sleep (**H**) during ZT 3 - 5 exposure to yellow or blue light stimulation. Paired t-test ($n = 9$). **I** The average duration of wakefulness, REM sleep, and NREM sleep during ZT 3 - 5 exposure to blue or yellow light stimulation. Paired t-test ($n = 9$).

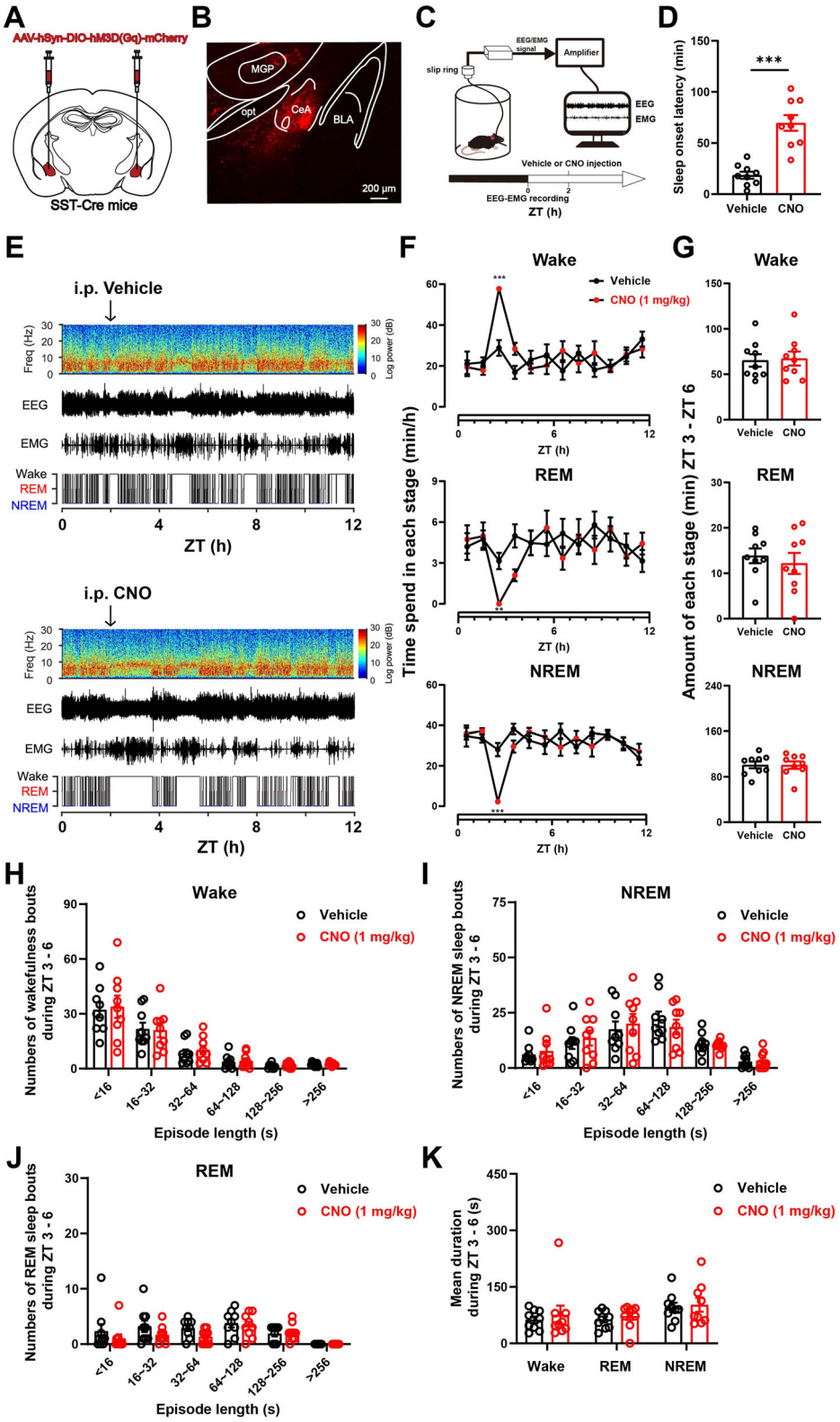

Fig. 4 | Effects of chemogenetic activation of CeA $^{SST+}$ neurons on sleep-wake behavior in mice. **A** Schematic diagram of AAV-hSyn-DIO-hM3D(Gq)-mCherry injection into the CeA of SST-Cre mice. **B** Representative image showing the expression of AAV-hSyn-DIO-hM3D(Gq)-mCherry in the CeA. Scale bars: 200 μm. **C** Schematic diagram of chemogenetic stimulation in sleep-wake behavior recording experiment. Mice were intraperitoneally injected with vehicle or CNO (1 mg/kg) at ZT 2. **D** Sleep latency after vehicle or CNO (1 mg/kg) injection at ZT 2. Paired t-test ($n = 9$). **E** Representative EEG power spectra, EEG/EMG traces and hypnogram after intraperitoneally injected with vehicle (top) or CNO (bottom). **F** Time course of wakefulness, NREM sleep, and REM sleep after vehicle or CNO intraperitoneal injection at ZT 2. Two-way repeated-measures ANOVA, Bonferroni post-hoc comparison ($n = 9$). **G** Total time spent in each stage during the ZT 3 - 6 after intraperitoneal injection of vehicle or CNO. Paired t-test ($n = 9$). The numbers of different episode lengths including wakefulness (**H**), NREM sleep (**I**) and REM sleep (**J**) during ZT 3 - 6 after vehicle and CNO (1 mg/kg) injection. Paired t-test ($n = 9$). **K** The average duration of wakefulness, REM sleep, and NREM sleep during ZT 3 - 6 after vehicle and CNO (1 mg/kg) injection. Paired t-test ($n = 9$).

(Fig. 7B, Vehicle vs. CNO, 51.03 ± 4.032 min vs. 27.37 ± 5.203 min), manifesting as increased EEG amplitude and decreased EEG activity (Fig. 7C). The CNO injection reduces the amount of wakefulness and increases the amount of NREM sleep in the first hour (Fig. 7D). To clarify the potential non-specific effects of CNO on stress-induced sleep-onset insomnia, we conducted a control experiment involving a cage change challenge, in which AAV-hSyn-DIO-hM4D(Gi)-mCherry was injected into the CeA of wild-type mice. The results revealed no significant change in sleep architecture or latency between the CNO and vehicle groups. Additionally, there were no change in the EEG power spectra between this two groups (Supplementary Fig. 10).

Previous studies have shown that stress before sleep can contribute to sleep-onset insomnia[23–25]. We exposed the mice to restraint stress before they entered the inactive phase to mimic the sleep-onset insomnia induced

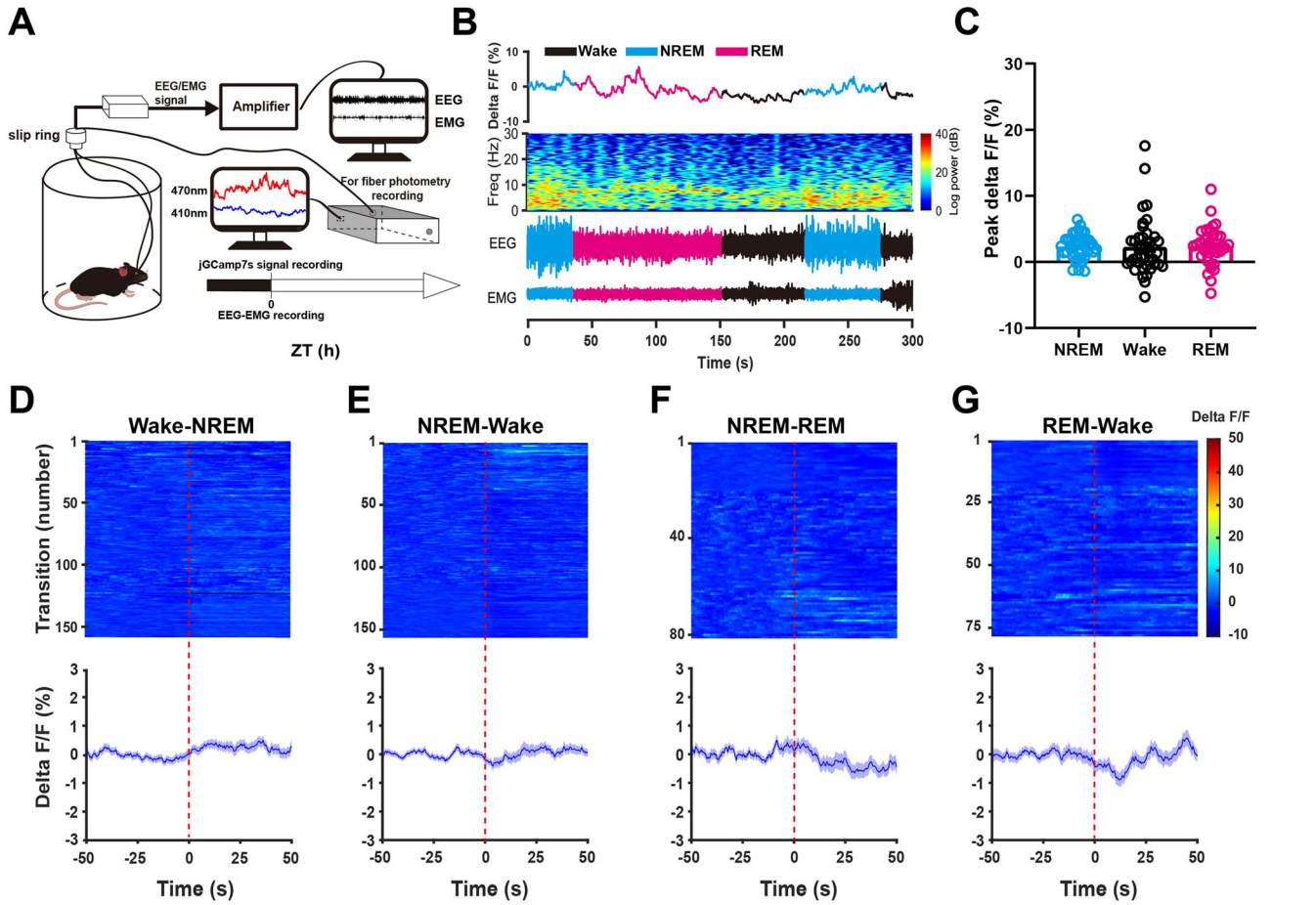

Fig. 5 | Population activity of CeA^{SST+} neurons across spontaneous sleep-wake behavior. A Schematic of experimental setup and workflow for fiber photometry recording. **B** Representative fluorescent traces, relative EEG power, and EEG/EMG traces across spontaneous sleep-wake behavior. **C** Ca^{2+} activity ($\Delta F/F$) peaks during wakefulness, NREM sleep, and REM sleep. one-way ANOVA ($n = 40$ from 4 mice). The Ca^{2+} activity of CeA^{SST+} neurons during transitions from wakefulness to NREM (**D**), NREM to wakefulness (**E**), NREM to REM (**F**), and REM to wakefulness (**G**). Heatmaps showing the intensity of Ca^{2+} signals across state transitions (top), the plot showing the average Ca^{2+} activity before and after 50 s of state transitions (bottom). Red vertical dashed lines indicate the time points of state transitions. $n = 158$ trials (**D**), 156 trials (**E**), 81 trials (**F**) and 78 trials (**G**) from 4 mice.

by pre-sleep stress. The mice subjected to restraint stress exhibited disrupted sleep homeostasis, primarily manifested by prolonged sleep latency (Supplementary Fig. 11). Next, we determine whether CeA^{SST+} neurons are necessary for restraint stress-induced sleep-onset insomnia. We found that inhibition of CeA^{SST+} neurons shortened sleep-onset latency induced by restraint stress (Supplementary Fig. 12). Taken together, these results revealed that the inhibition of CeA^{SST+} neurons alleviated the acute stress-induced sleep-onset insomnia.

Discussion

Insomnia is a prevalent mental health issue that contributes to various physical and mental illnesses[26]. Therefore, it is imperative to explore its etiology and pathological mechanisms. In addition to distinctive symptoms, different insomnia subtypes exhibit diverse electroencephalogram biomarkers, developmental trajectories, comorbidities, and responses to treatment[27]. This evidence implies that insomnia subtypes may not share common pathogenic mechanisms. Compared to sleep maintenance difficulties, sleep-onset difficulties may serve as a "gateway" symptom to stubborn and complex insomnia[2]. Considering the high prevalence of occasional or persistent sleep-onset difficulties and the limited therapeutic options available[28], identifying neural substrates regulating sleep-onset insomnia holds significant clinical importance.

In this study, although we delivered a 3 h laser to activate CeA^{SST+} neurons of SST-Cre mice, we only observed an increased wakefulness in the first hour, with no significant change in the remaining two hours. Similarly, chemogenetic activation of CeA^{SST+} neurons resulted in heightened wakefulness during the initial hour. Despite being a relatively chronic activation method, chemogenetics theoretically induces a more pronounced wake-promoting effect. However, neither optogenetic nor chemogenetic activation of CeA^{SST+} neurons led to a substantial increase in wakefulness upon closer examination. Furthermore, analysis of wakefulness, NREM sleep, and REM sleep episodes revealed that CeA^{SST+} neurons do not affect sleep maintenance. These results suggest that CeA^{SST+} neurons may primarily regulate sleep latency rather than wake or sleep maintenance. Over-excitation of the CeA^{SST+} neurons may, at least in part, contribute to the pathogenesis of sleep-onset insomnia.

Stress is one of the major causes of sleep-onset insomnia, and exposure to stressors will lead to difficulty in falling asleep[22,23]. In our present study, we adopted two models, cage change challenge and physical restraint, to investigate the regulatory role of CeA^{SST+} neurons in stress-induced sleep-onset insomnia and post-stress sleep-onset insomnia, respectively. The cage change challenge serves as an insomnia model to mimic the "first night effect" of transient insomnia, which is a well-known phenomenon resulting from maladaptation to an unfamiliar sleep environment[29]. The first night effect is characterized by a longer sleep-onset latency, an increase of nocturnal wakefulness, and a decrease of total sleep time[30,31]. Consistent with the manifestation of first night effect, animal experimental results have shown that the cage change challenge lengthens the sleep-onset latency and increases the total wakefulness in mice[32]. In this study, chemogenetic inhibition of CeA^{SST+} neurons

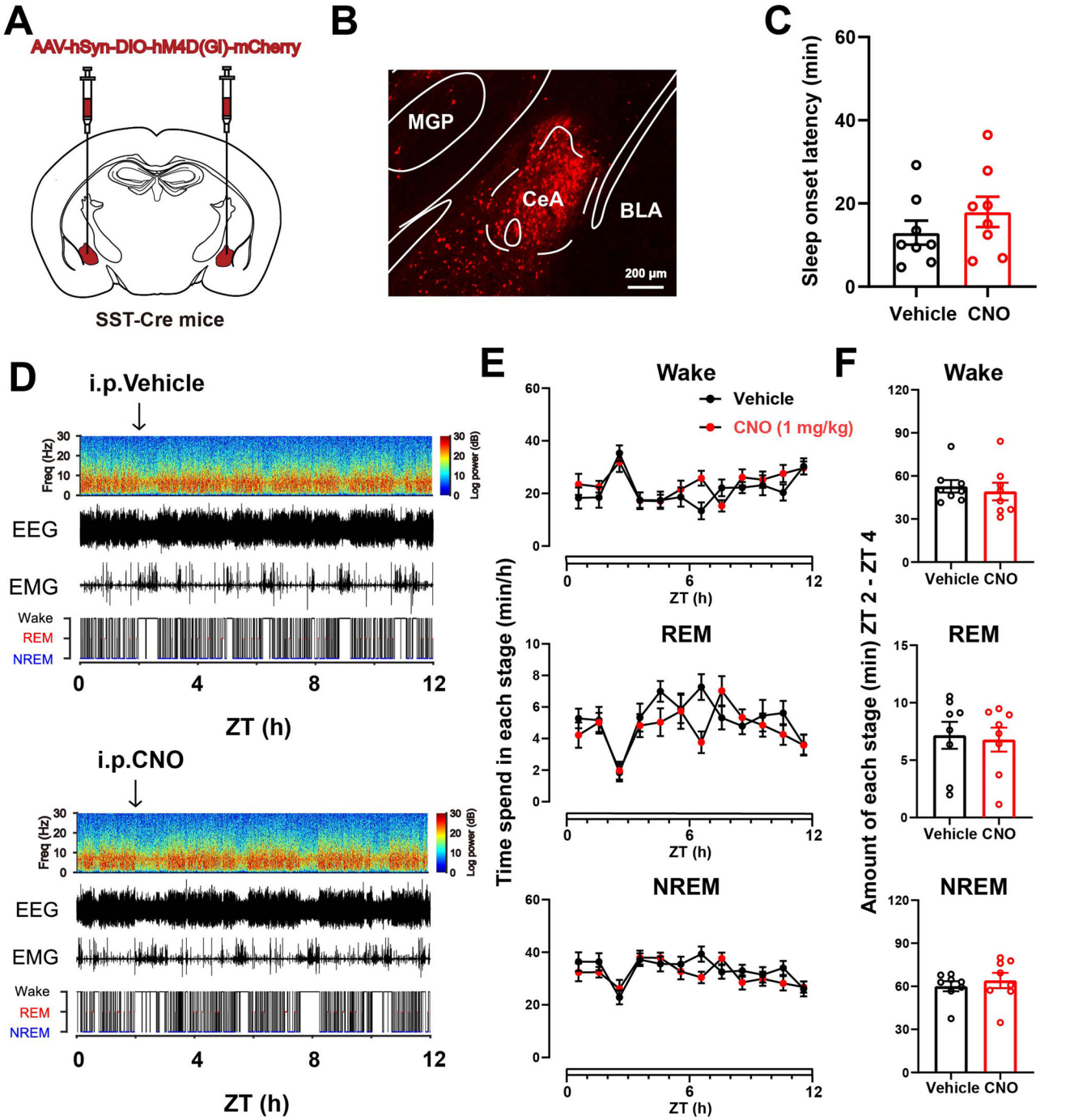

Fig. 6 | Effects of chemogenetic inhibition of CeA $^{SST+}$ neurons on sleep architecture in physiological conditions. **A** Schematic diagram of AAV-hSyn-DIO-hM4D(Gi)-mCherry injection into CeA. **B** Representative image showing the expression of AAV-hSyn-DIO-hM4D(Gi)-mCherry in the CeA. Scale bars: 200 μm. **C** Sleep latency after vehicle or CNO (1 mg/kg) injection at ZT 2. Paired t-test ($n = 8$). **D** Representative EEG power spectra, EEG/EMG traces and hypnogram after vehicle (top) or CNO (bottom) injected. **E** Time course of wakefulness, NREM sleep, and REM sleep following vehicle or CNO injection at ZT 2. Two-way repeated-measures ANOVA, Bonferroni post-hoc comparison ($n = 8$). **F** Total time spent in each stage 2 h after intraperitoneal injection of vehicle or CNO. Paired t-test ($n = 8$).

shortened sleep-onset latency, and only reduced 1st hour wakefulness during the cage change challenge, indicating that the inhibition of CeA^{SST+} neurons alleviates the sleep-onset insomnia symptoms triggered by the cage change challenge. In addition, the restraint model is another typical model of stress-induced sleep-onset insomnia, the representative phenotype of which contains significantly prolonged sleep-onset latency and slightly disrupted sleep architecture[24,33] and is consistent with our restraint model results. Our experimental results revealed that chemogenetic inhibition of CeA^{SST+} neurons significantly shortened the sleep latency induced by restraint stress, which indicates the amelioration of restraint stress-induced sleep-onset insomnia after the inhibition of CeA^{SST+} neurons. Therefore, we speculate that CeA^{SST+} neurons play an important role in alleviating sleep-onset insomnia caused by stress, which represents a potential therapeutic target for stress-induced sleep-onset insomnia. Notably, our results indicate that the inhibition of CeA^{SST+} neurons does not interrupt physiological sleep-wake behavior, rendering CeA^{SST+} neurons an ideal target for the development of novel anti-insomnia drugs with low adverse effects on natural sleep.

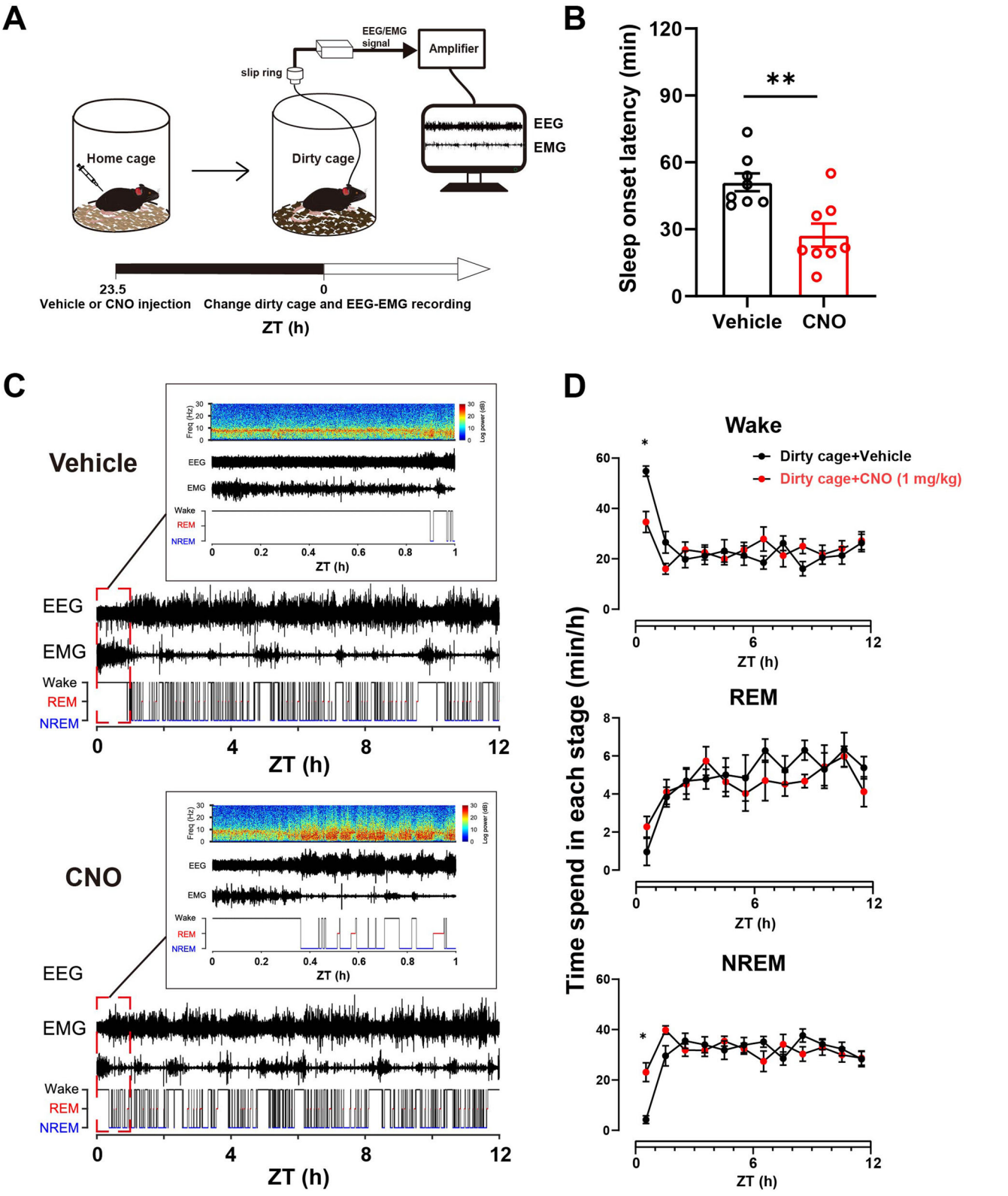

Fig. 7 | Effects of chemogenetic inhibition of CeA^{SST+} neurons in acute cage changing stress condition. A Schematic diagram of sleep recording experiment after exposure to cage changing stress. **B** Sleep latency after vehicle or CNO (1 mg/kg) injection in cage change challenge. Paired t-test ($n = 8$). **C** Representative EEG power spectra, EEG/EMG traces and hypnogram after vehicle (top) or CNO (bottom) injection in cage change challenge-induced acute stress condition. **D** Time course of wakefulness, NREM sleep, and REM sleep after vehicle or CNO injection in cage change challenge. Two-way repeated-measures ANOVA, Bonferroni post-hoc comparison ($n = 8$).

Our results suggest that CeA^{SST+} neurons are involved in the regulation of stress-induced sleep-onset insomnia, but the specific neural regulatory network underlying this process is not yet clear. On the one hand, the CeA receives modulatory inputs from various cortical, thalamic, hypothalamic, and brainstem regions, such as PVT and VTA[34]. We injected AAV-CaMKIIa-EGFP and AAV-CaMKIIa-mCherry into the PVT and VTA nuclei of wild-type mice, respectively. Immunohistochemical analysis revealed the presence of glutamatergic projections from both the PVT and VTA nuclei within the CeA, with some overlap observed with SST+ neurons. Additionally, we noted spatial differences in the distribution of glutamatergic projections from these two regions within the CeA (Supplementary Fig. 13). Recent studies from our lab have shown that acute activation of CeA-projecting VTA glutamatergic neurons caused arousal and defensive behaviors[35]. In addition, studies from Zhao et al. showed that the calcium activity of CeA-projecting PVT neurons rapidly increased in response to stressful events, and optogenetic activation of the PVT-CeA circuit prompted the transition from NREM sleep to wakefulness, while chemogenetic inhibition of CeA-projecting PVT neurons alleviated sleep-onset insomnia triggered by acute stressors such as restraint and cage change challenge[24]. These findings suggest that CeA^{SST+} neurons may regulate stress-induced sleep-onset insomnia through upstream VTA and PVT glutamatergic neurons. On the other hand, the CeA sends inhibitory outputs to various sleep-wake regulation regions, including the basal forebrain, thalamus, hypothalamus, and brainstem[34,36]. It is conceivable that CeA^{SST+} neurons may promote wakefulness via suppressing downstream sleep-promoting neural substrates, where ventrolateral periaqueductal gray (vlPAG) is a promising target[37,38]. Recent studies have shown that optogenetic inhibition of neurotensin (NTS)-expressing glutamatergic neurons in vlPAG induced the transition from NREM sleep to wakefulness, while chemogenetic inhibition increased wakefulness[39]. It is possible that CeA^{SST+} neurons may induce arousal, at least partially, through inhibiting downstream NTS-expressing glutamatergic neurons in vlPAG. In the future, it is necessary to further elucidate the upstream and downstream neural targets and circuits underlying stress-induced insomnia.

In conclusion, our research results reveal that CeA^{SST+} neurons are activated in response to acute stressors and participate in the regulation of stress-induced sleep-onset insomnia. However, CeA^{SST+} neurons are not essential for the spontaneous sleep-wake behavior. Moving forward, therapeutic interventions targeting CeA^{SST+} neurons may offer a promising avenue for treating acute stress-related sleep-onset insomnia effectively, without disturbing the basal sleep.

Methods and materials

Animals

SST-Cre mice were kindly provided by Dr.Tao Tan (Wenzhou Medical University). C57BL/6 mice were obtained from Guangdong GemPharmatech Co., Ltd. Adult C57BL/6 mice and SST-Cre mice, with randomized gender distribution, were used in this study, and all animals were 8–12 weeks old and weighed about 22–28 g. Animals were randomly assigned to experimental and control groups using a random number. Mice were housed in a suitable and ventilated environment which includes a temperature-and humidity-controlled animal facility and a 12-h/12-h light/dark cycle (light on at clock time 07:00 - 19:00). The mice had allowed free access to food and water. One week before the behavioral tests and polysomnography recording, mice were single housed and kept on a 12-h reverse light/dark cycle (light on from zeitgeber time (ZT) 0 to ZT 12, ZT 0 is related to clock time 19:00). We have complied with all relevant ethical regulations for animal use. This study was approved by the animal ethics committee of the Fujian Medical University (IACUC FJMU 2023-0270).

Stereotaxic surgery and virus injection

Before craniotomy surgery, the mice were anesthetized with 3% isoflurane in an induction box. Afterward, the mice were fixed on a stereotaxic apparatus and the isoflurane was kept at 1% during the anesthesia process. Erythromycin eye cream was used to protect mice's eyes from dryness and light. After exposing the skull and adjusting level balance, we drilled a small hole in the skull for virus injection by referring to the position coordinates in Paxinos & Watson mouse brain stereotaxic map. CeA (bregma, AP = −1.20 mm, ML = ± 2.7 mm, DV = −4.90 mm) was injected with 200 nL of virus bilaterally at a rate of 40 nL/min. After virus injection, the needle was abided for 10 min for virus diffusion. Then the needle was slowly pulled out at a constant speed. To record the calcium (Ca^{2+}) activity of CeA^{SST+} neurons, Cre-dependent AAV-EF1a-DIO-GCamp7s (BrainVTA Technology) was injected into the CeA. To activation of CeA^{SST+} neuronal soma in the CeA, AAV-EF1a-DIO-hChR2(H134R)-mCherry or AAV-hSyn-DIO-hM3D(Gq)-mCherry were injected into the CeA in SST-Cre mice. In order to inhibit the CeA^{SST+} neurons by chemogenetics, AAV-hSyn-DIO-hM4D(Gi)-mCherry was injected into the CeA of SST-Cre mice. Afterward, electrodes for electroencephalography (EEG)/electromyography (EMG) recording and optical fibers were implanted, based on experimental requirements. After surgery, the mice were placed in a 37°C incubator until they were fully recovered, and then transferred to their home cage where food and water were constantly available. AAV-EF1a-DIO-GCamp7s, AAV-EF1a-DIO-hChR2(H134R)-mCherry, AAV-hSyn-DIO-hM3D(Gq)-mCherry, and AAV-hSyn-DIO-hM4D(Gi)-mCherry, were purchased from BrainVTA (China) or Taitool Bioscience (China).

Fiber photometry recording

After about 3–4 weeks of recovery from surgery, mice were connected to the fiber photometry recording system for jGCaMP7s signal recording (Inper Technology, China). The instrument is equipped with 470 nm and 410 nm excitation lasers, where the 470 nm laser is used to excite jGCaMP7s fluorescence signals and 410 nm laser is used as a control for fluorescence bleaching. jGCaMP7s signal was sampled at 30 Hz. The raw data were processed using a MATLAB R2019b script offered by the provider company. The change of Ca^{2+} signal was calculated with the formula of $\Delta F/F = (F-F0)/F0$, where F0 was the average fluorescence signal value during baseline in each test. The $\Delta F/F$ values are shown with a peri-event heatmap and a plot of the average Ca^{2+} transients, and the shaded area represents the standard error (SEM).

In the stress stimuli experiments, we exposed the mice to restraint, air puff and rat bedding stimuli, and all experiments were conducted during the dark phase (ZT 12 - ZT 24). In these stimuli experiments, the jGCaMP7s fluorescence signals were analyzed from −5 s to 20 s of stress stimuli. For cage change experiments, the change of jGCaMP7s signals was analyzed 60 s before (defined as baseline) and 180 s after the event. The jGCaMP7s signals of CeA^{SST+} neurons across spontaneous sleep-wake behavior were collected between ZT 0 and ZT 5. All state transitions were judged by EEG/EMG activity. The Ca^{2+} activity of CeA^{SST+} neurons was analyzed from 50 s before to 50 s after related phase transition.

Acute stress protocols

Restraint. Mice were restrained by a trained experimenter. In the optical fiber recording experiment, the mice were restricted by the experimenter's right hand for 5 s, and each mouse was restricted 8–10 times. In sleep recording experiments, the mice were confined to a 50 mL centrifuge tube. After 1 h of restraint, the mice were immediately released from the tube and placed back in their home cage[24].

Rat bedding. The mice were exposed to a rat bedding on a small petri dish for 5 s[33]. Each mouse was exposed 8–10 times.

Air puff. Before exposure to stressor, the mice adapted to the sound emitted by the blowing device for 2 min, and then received the air puff for 5 s[40]. Each mouse was exposed 8-10 times.

Cage change challenge. After getting used to the experimenter's handling, mice were subjected to cage change challenge. The mice were gently transferred from their home cage to a dirty cage where

other mice who was not a littermate had lived for at least seven days[41]. Each mouse was exposed 8–10 times at 5–10 min intervals.

Acute stress-induced insomnia model. We conducted acute stress model using the cage change and restraint method described before[33,41,42]. In the restraint experiments, EEG/EMG signals were recorded during the light period (ZT 0 - ZT 12) on the first day. On the second day, EEG/EMG signals were recorded during the light period (ZT 0 - ZT 12) after 1 h of restraint in 50 mL tube. In the cage change experiment, the mice were transferred from their home cage to a dirty cage inhabited by mice from other litters for at least 7 days. Briefly, the mice were placed in their home cage from ZT 0 to ZT 24 on the first day, and transferred to the dirty cage at ZT 0 on the second day, and their EEG/EMG signals were recorded from ZT 0 to ZT 12. The mice moved freely and had ad libitum access to food and water throughout the whole experiments.

Pupil size recording and analysis. Pupil size was recorded in anesthetized and head fixed mice. Isoflurane was used to anesthetize mice. After the disappearance of the righting reflex, the mice were fixed into a stereotaxic apparatus, and 1.2% isoflurane was continuously administered at a flow rate of 1.0 L/min. The infrared camera was fixed in position to face pupil of mice. When the pupil remained constricted between the two eyelids, images were acquired for a duration of 7 min. Blue light stimulation (10 ms, 30 Hz, 3–5 mW/mm^2, 1 min) was administered at the beginning of the 4th minute. The image acquisition rate was adjusted into 30 Hz and the size of pupil was analyzed using an open-source software Bonsai (http://bonsai-rx.org/). The average pupil size in 1 min before blue light stimulation served as the base value. Data are represented as relative values of pupil size (the diameters of the pupil size divided by the base value). The relative values were corrected using the mean filtering algorithm.

Respiratory rate recording and analysis. Mice were placed in the plethysmography chamber of a whole-body plethysmograph (WBP-4M, TOW-INT TECH, China). 1.2% isoflurane was continuously injected into the chamber at a flow rate of 1.0 L/min. After anesthesia and respiratory status were stabilized, tidal volume (Vt) was record and respiratory rate was calculated by software (ResMass 1.4.2, TOW-INT TECH, China) for 3 min. Blue light stimulation to mice was started at the 2nd min (10 ms, 30 Hz, 3-5 mW/mm^2, 1 min).

Anxiety-like behavior test. Two standard behaviors were used to evaluate anxiety-like behavior in mice, including the open field test (OFT) and elevated plus maze (EPM). A square acrylic box (45 × 45 × 45 cm, 15 × 15 cm square center defined as the center) was used for the OFT. The EPM test consists of 2 open arms (30 × 5 cm, with 1 cm ledges) and 2 closed arms (30 × 5 cm, with 15 cm walls) with a height of 50 cm to the floor. After 10 min of optical fiber adaptation, the mice were placed in the central area of the OFT and EPM with their backs to the experimenter. At the same time, the mice were given blue or yellow light stimulation (473 nm/589 nm, 10 ms, 20 Hz, 3 s on, 2 s off, 3–5 mW/mm^2 for 5 min). The movements of the mice were recorded by infrared cameras and quantified by Smart software.

Polysomnographic recordings and analysis. Prior to the recording and experimental procedures, the mice are placed individually in transparent glass containers and housed within an insulated soundproof recording chamber. The cables are connected to a slip ring unit, allowing unrestricted movement of the mice, which are given an adjustment period of 3–4 days to alleviate stress. The EEG and EMG signals are amplified, band-pass filtered (EEG: 0.5–30 Hz; EMG: 20–200 Hz), digitized at a sampling rate of 128 Hz and recorded using Vital Recorder software (Kissei Comte, Japan). The SleepSign3.0 software is utilized to analyze the sleep states. Wakefulness is defined as low-amplitude EEG activity with high levels of muscle activity. NREM sleep is defined as synchronous, high-amplitude, low-frequency (0.5–4 Hz) EEG signals without any EMG activity. REM sleep is defined by prominent theta-like (4–9 Hz) EEG activity and muscle relaxation. The data is segmented into 4-second epochs and automatically analyzed. Manual calibration is required if necessary.

Optogenetic stimulation during polysomnographic recordings. Before the optogenetic stimulation experiment, mice need to adjust their circadian rhythm and adapt to the environment for one week. A short-term blue light (473 nm, 10 ms, 3–5 mW/mm^2) or yellow light (589 nm, 10 ms, 3–5 mW/mm^2) stimulation test was conducted to observe the possibility of state transition and the latency. Different frequency stimulations at 0, 5, 10, 20, and 40 Hz were given at least 20 s after the NREM state, and the time required for wakefulness under each frequency stimulation was recorded. At least three stimulation events were recorded at each frequency, and the average was calculated. Long-term stimulation experiments were conducted during the ZT 2 - ZT 3 or ZT 2 - ZT 5 using a semi-chronic light stimulation protocol (10 ms, 20 Hz, 3–5 mW/mm^2, 30 s light on and 30 s light off). Throughout the entire experimental process, the mice were ensured unrestricted movement and had sufficient access to food and water.

Chemogenetics in the polysomnographic recording experiments. In the physiological sleep experiment, after adjusting the circadian rhythm of the SST-Cre mice and adapting them to the environment, intraperitoneal injections of vehicle or CNO (1 mg/kg) were administered at ZT 2. EEG and EMG signals were recorded to analyze the changes in sleep latency and sleep duration in mice after intraperitoneal injections. Stable sleep was defined as continuous sleep for more than 20 s. For the inhibition of cage change stress-induced insomnia in mice, vehicle or CNO (1 mg/kg) was intraperitoneally injected half an hour before the cage change challenge at the ZT 0. EEG and EMG signals were recorded from ZT 0 to ZT 12.

For the inhibition of restraint stress-induced insomnia in mice, vehicle or CNO (1 mg/kg) was intraperitoneally injected at ZT 22.5. At ZT 23, the mice were subjected to restraint for 1 h and then released back into their home cage at the beginning of the light cycle. EEG and EMG signals were recorded from ZT 0 to ZT 12.

Histology and immunohistochemistry. Mice were deeply anesthetized with sodium pentobarbital and perfused with 0.01 M phosphate-buffered saline (PBS) followed by 4% paraformaldehyde. After decapitation, the brains were removed and immersed in 4% paraformaldehyde for 24 h. The brains were then dehydrated in 20% and 30% sucrose solutions for 24 h sequentially and sectioned into 30 μm slices using a cryostat. For immunofluorescence, brain slices were permeabilized with 0.7% Triton X-100 (TB210 Solarbio) at 37 °C for 1 h. The slices were then incubated with the primary antibody solution (rabbit anti-c-fos, 1:1000, ab190289, Abcam; rabbit anti-SST, 1 :1000, PA5-85759, Thermo Fisher Scientific) for 24 h. Subsequently, the slices were placed in the secondary antibody solution (Alexa Fluor 488 goat anti-rabbit, 1:1000, 111-545-003, Jackson Laboratory; Alexa Fluor 647 goat anti-rabbit, 1:1000, 111-605-003, Jackson Laboratory) and incubated at 37 °C for 2 h. After washing, the slices were stained with DAPI solution (1:50, Beyotime Biotechnology) to label cell nuclei. Finally, the images were captured using an inverted fluorescence microscope and processed using LAX and Adobe Photoshop software.

Statistics and reproducibility. All data are presented as mean ± SEM. Statistical analysis was performed using paired t-test and two-way ANOVA with Bonferroni post-hoc test in Graphpad 8.0 software. If the data did not pass the Shapiro-Wilk normality test, non-parametric analysis methods were used. Statistical significance is indicated as $^*p < 0.05$, $^{**}p < 0.01$, $^{***}p < 0.001$. The layout of all figures was generated by Adobe Illustrator 2020.

Reporting summary

Further information on research design is available in the Nature Portfolio Reporting Summary linked to this article.

Data availability

Numerical source data for all graphs in the manuscript can be found in the supplementary data file. We have also deposited the data files on Dryad and the corresponding DOI is https://doi.org/10.5061/dryad.6djh9w19b.

Received: 13 June 2024; Accepted: 3 February 2025;
Published online: 06 March 2025

References

1. Kocevska, D. et al. Sleep characteristics across the lifespan in 1.1 million people from the Netherlands, United Kingdom and United States: a systematic review and meta-analysis. *Nat. Hum. Behav.* **5**, 113–122 (2021).
2. Pillai, V. et al. The nature of stable insomnia phenotypes. *Sleep* **38**, 127–138 (2015).
3. Zolfaghari, S. et al. Effects of menopause on sleep quality and sleep disorders: Canadian Longitudinal Study on Aging. *Menopause* **27**, 295–304 (2020).
4. Staner, L. et al. A new sublingual formulation of zolpidem for the treatment of sleep-onset insomnia. *Expert Rev. Neurother.* **12**, 141–153 (2012).
5. Cappuccio, F. P. et al. Sleep and cardio-metabolic disease. *Curr. Cardiol. Rep.* **19**, 110 (2017).
6. Baron, K. G. et al. Circadian misalignment and health. *Int. Rev. Psychiatry* **26**, 139–154 (2014).
7. Alnawwar, M. A. et al. The effect of physical activity on sleep quality and sleep disorder: a systematic review. *Cureus* **15**, e43595 (2023).
8. Cano, G. et al. Neural circuitry of stress-induced insomnia in rats. *J. Neurosci.* **28**, 10167–10184 (2008).
9. Wang, Y. et al. Multimodal mapping of cell types and projections in the central nucleus of the amygdala. *Elife* **12**, e84262 (2023).
10. Ma, C. et al. Sleep regulation by neurotensinergic neurons in a thalamo-amygdala circuit. *Neuron* **103**, 323–334 (2019).
11. Snow, M. B. et al. GABA cells in the central nucleus of the amygdala promote cataplexy. *J. Neurosci.* **37**, 4007–4022 (2017).
12. Mahoney, C. E. et al. GABAergic neurons of the central amygdala promote cataplexy. *J. Neurosci.* **37**, 3995–4006 (2017).
13. Li, H. et al. Experience-dependent modification of a central amygdala fear circuit. *Nat. Neurosci.* **16**, 332–339 (2013).
14. Li, B. Central amygdala cells for learning and expressing aversive emotional memories. *Curr. Opin. Behav. Sci.* **26**, 40–45 (2019).
15. Nanda, S. A. et al. Predator stress induces behavioral inhibition and amygdala somatostatin receptor 2 gene expression. *Genes Brain Behav.* **7**, 639–648 (2008).
16. Chen, W. H. et al. Neuronal basis for pain-like and anxiety-like behaviors in the central nucleus of the amygdala. *Pain* **163**, e463–e475 (2022).
17. Jo, Y. S. et al. Persistent activation of central amygdala CRF neurons helps drive the immediate fear extinction deficit. *Nat. Commun.* **11**, 422 (2020).
18. Tye, K. M. et al. Amygdala circuitry mediating reversible and bidirectional control of anxiety. *Nature* **471**, 358–362 (2011).
19. Sanford, L. D. et al. Stress, arousal, and sleep. *Curr. Top Behav. Neurosci.* **25**, 379–410 (2015).
20. Li, Y. D. et al. Ventral pallidal GABAergic neurons control wakefulness associated with motivation through the ventral tegmental pathway. *Mol. Psychiatry* **26**, 2912–2928 (2021).
21. Tossell, K. et al. Somatostatin neurons in prefrontal cortex initiate sleep-preparatory behavior and sleep via the preoptic and lateral hypothalamus. *Nat. Neurosci.* **26**, 1805–1819 (2023).
22. Marcusson-Clavertz, D. et al. Relationships between daily stress responses in everyday life and nightly sleep. *J. Behav. Med.* **45**, 518–532 (2022).
23. Maclean, R. R. et al. The relationship between anxiety and sleep-wake behavior after stressor exposure in the rat. *Brain Res.* **1164**, 72–80 (2007).
24. Zhao, J. et al. A paraventricular thalamus to central amygdala neural circuit modulates acute stress-induced heightened wakefulness. *Cell Rep.* **41**, 111824 (2022).
25. Morin, C. M. et al. Role of stress, arousal, and coping skills in primary insomnia. *Psychosom Med.* **65**, 259–267 (2003).
26. Fernandez-Mendoza, J. et al. Insomnia and its impact on physical and mental health. *Curr. Psychiatry Rep.* **15**, 418 (2013).
27. Blanken, T. F. et al. Insomnia disorder subtypes derived from life history and traits of affect and personality. *Lancet Psychiatry* **6**, 151–163 (2019).
28. Morin, A. K. et al. Therapeutic options for sleep-maintenance and sleep-onset insomnia. *Pharmacotherapy* **27**, 89–110 (2007).
29. Qu, W. M. et al. Essential role of dopamine D2 receptor in the maintenance of wakefulness, but not in homeostatic regulation of sleep, in mice. *J. Neurosci.* **30**, 4382–4389 (2010).
30. Agnew, H. W. Jr et al. The first night effect: an EEG study of sleep. *Psychophysiology* **2**, 263–266 (1966).
31. Coates, T. J. et al. First night effects in good sleepers and sleep-maintenance insomniacs when recorded at home. *Sleep* **4**, 293–298 (1981).
32. Islam, M. T. et al. Vasopressin neurons in the paraventricular hypothalamus promote wakefulness via lateral hypothalamic orexin neurons. *Curr. Biol.* **32**, 3871–3885 (2022).
33. Li, S. B. et al. Hypothalamic circuitry underlying stress-induced insomnia and peripheral immunosuppression. *Sci. Adv.* **6**, eabc2590 (2020).
34. Moscarello, J. M. et al. The central nucleus of the amygdala and the construction of defensive modes across the threat-imminence continuum. *Nat. Neurosci.* **25**, 999–1008 (2022).
35. Chen, S. Y. et al. Control of behavioral arousal and defense by a glutamatergic midbrain-amygdala pathway in mice. *Front. Neurosci.* **16**, 850193 (2022).
36. Liu, J. et al. Differential efferent projections of GABAergic neurons in the basolateral and central nucleus of amygdala in mice. *Neurosci. Lett.* **745**, 135621 (2021).
37. Sun, Y. et al. Amygdala GABA Neurons Project To vlPAG And mPFC. *IBRO Rep.* **6**, 132–136 (2019).
38. Penzo, M. A. et al. Fear conditioning potentiates synaptic transmission onto long-range projection neurons in the lateral subdivision of central amygdala. *J. Neurosci.* **34**, 2432–2437 (2014).
39. Zhong, P. et al. Control of Non-REM Sleep by Midbrain Neurotensinergic Neurons. *Neuron* **104**, 795–809.e796 (2019).
40. Yuan, Y. et al. Reward Inhibits Paraventricular CRH Neurons to Relieve Stress. *Curr. Biol.* **29**, 1243–1251.e1244 (2019).
41. Machado, N. L. S. et al. Median preoptic GABA and glutamate neurons exert differential control over sleep behavior. *Curr. Biol.* **32**, 2011–2021.e2013 (2022).
42. Zimprich, A. et al. A robust and reliable non-invasive test for stress responsivity in mice. *Front. Behav. Neurosci.* **8**, 125 (2014).

Acknowledgements

We thank Dr.Tao Tan (Wenzhou Medical University) for providing the SST-Cre mice. This study was supported by the following grants: the National Natural Science Foundation of China (82271529 to P.C., 82471503 to L.C.); Joint Funds for the Innovation of Science and Technology in Fujian Province, China (2021Y9005 to L.C.); The Natural Science Foundation of Fujian Province, China (2024J01582 to P.C.); Fujian Key Laboratory of Drug Target Discovery and Structural and Functional Research, Fujian Medical University (FKLDSR-202304 to P.C.).

Author contributions

Experimental design: P.C., L.C., and W.Y.; Stereotaxic surgery: W.Y., S-X.H., and L.Z.; Fiber photometry recording: W.Y., D-Y.H., K-Q.H., and Z-X.H.; EEG/EMG recordings: W.Y., S-X.H., Z-S.L., D-Y.H., K-Q.H., Z-X.H., L-W.N., and J-L.L.; Immunohistochemical and microscopy procedures: W.Y., S-X.H., L.Z., and Z-S.L.; Data curation: W.Y., S-X.H., L.Z., Z-S.L., D-Y.H., K-Q.H., Z-X.H., L-W.N., and J-L.L.; Funding acquisition: P.C. and L.C.; Resources: P.C. and L.C.; Original manuscript preparation: W.Y., S-X.H., L.Z., and Z-S.L.; Review & editing writing: P.C. and L.C.

Competing interests

The authors declare no competing interests.

Additional information

Supplementary information The online version contains supplementary material available at https://doi.org/10.1038/s42003-025-07679-8.

Correspondence and requests for materials should be addressed to Li Chen or Ping Cai.

Peer review information *Communications Biology* thanks the anonymous reviewers for their contribution to the peer review of this work. Primary Handling Editor: Christina Karlsson Rosenthal.